TELKOMNIKA, Vol.13, No.1, March 2015, pp. 1~12
ISSN: 1693-6930, accredited A by DIKTI, Decree No: 58/DIKTI/Kep/2013
DOI: 10.12928/TELKOMNIKA.v13i1.1180

Variable Step Size Perturb and Observe MPPT for PV Solar Applications

Awang Bin Jusoh*[1], Omer Jamal Eldin Ibrahim Mohammed[2], Tole Sutikno[3]
[1,2] Faculty of Electrical Engineering, Universiti Teknologi Malaysia
81310 Johor Bahru, Malaysia
[3]Department of Electrical Engineering, Faculty of Industrial Technology, Universitas Ahmad Dahlan, Yogyakarta 55164, Indonesia
*Corresponding author, email: awang@fke.utm.my[1], omer.jamal.ibrahim@gmail.com[2], tole@ee.uad.ac.id[3]

Abstract

In order to deliver maximum output of photovoltaic (PV) cells, the usage of maximum power point tracking (MPPT) is essential. The speed and stability of the tracking technique are highly desired. Perturb and Observe (P&O) is one of the most common tracking techniques, but it suffers from the slow tracking speed at small duty cycle step and fluctuates when subjected with large duty step, which results in higher losses under dynamic weather to which the photovoltaic (PV) cells exposed. In this paper, variable step size Perturb and Observe is introduced throughout Matlab/Simulink simulation to overcome this problem to achieve higher efficiency, reliable tracking accuracy and higher speed under fast changing weather. In comparison with other variable P&O techniques, the proposed method features a dynamic step size for more tracking efficiency and accuracy. Double diode modelling is used in this technique for better photovoltaic (PV) cell's characteristic prediction. In this study, the adapted technique had been tested to wide range of sun irradiance and operation temperatures.

Keywords: *double diode modelling, PV solar, MPPT, perturb and observe, matlab/Simulink*

1. Introduction

PV cells are recognised for having non-linear characteristics. At one point, which is known as the maximum power point (MPP), the cells are capable to operate at maximum efficiency and give the maximum output [1]-[4]. Figure 1 shows the V-I and V-P characteristics of a typical 150W PV cell. The V-I and V-P can be distinguished from how their load is applied, either from short circuit to open circuit, i.e. from zero loads to infinity.

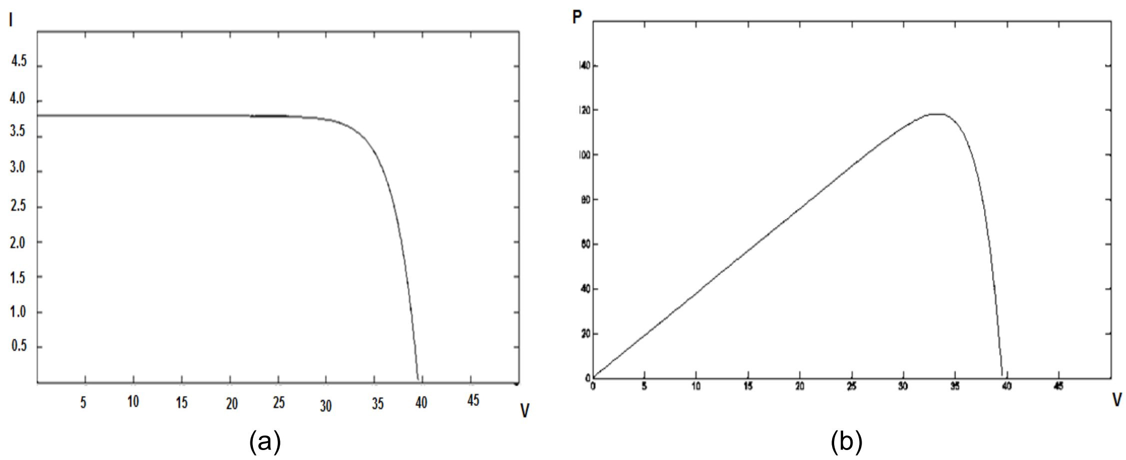

Figure 1. V-I and V-P characteristics of a typical 150W PV cell; (a). V-I (b). V-P

The point of maximum operation shifts with the changes of the sun irradiance, solar panel surface temperature and degree of the sun irradiance [5]. Figure 2 illustrates the V-I and

Received October 2, 2014; Revised January 4, 2015; Accepted January 15, 2015

V-P characteristics with respect to solar irradiance when the temperature is fixed. When the solar irradiance changes, the point of maximum shifts; for example, the PV cell output current decreases dramatically when the solar irradiance decreases. In Figure 3, it is noticeable that the increase of PV cell temperature causes a significant drop in the output voltage as well as output power.

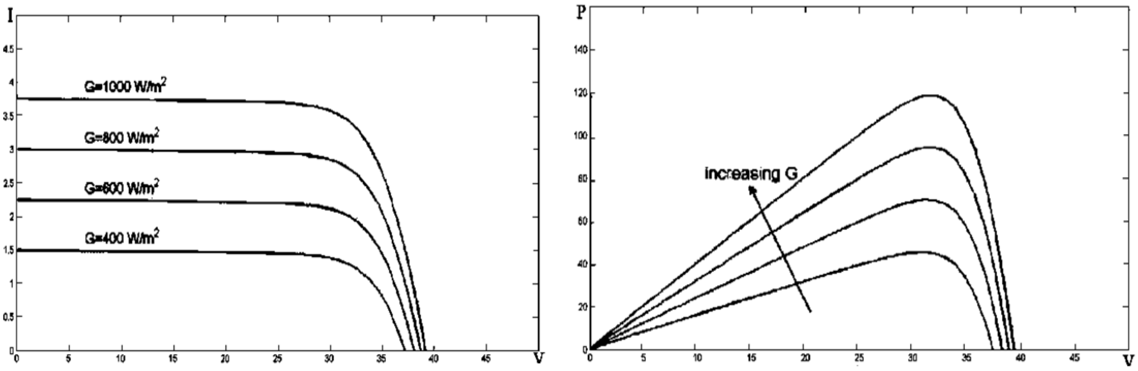

(a) (b)

Figure 2. V-I and V-P characteristics under variable radiations; (a). V-I (b). V-P

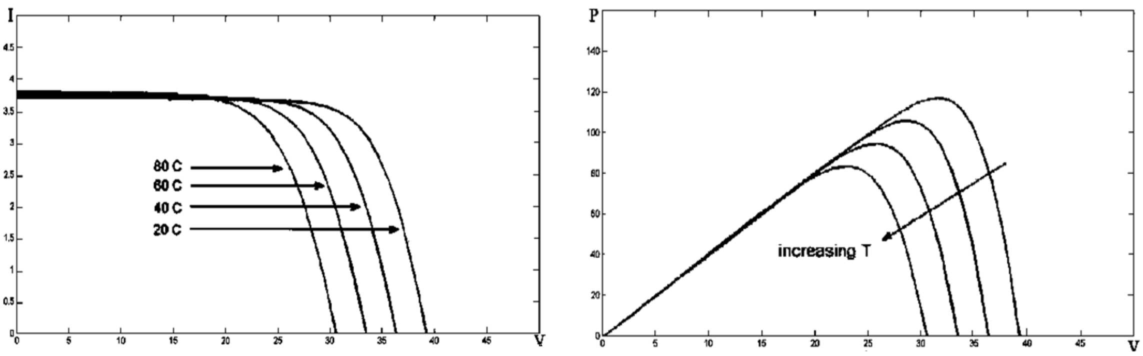

(a) (b)

Figure 3. V-I and V-P characteristics under variable temperature;(a). V-I (b). V-P

2. PV cell equivalent circuits

The PV cell can be modelled either using single diode for ease of calculation, or double diode for better accuracy, efficiency and prediction of the characteristics during partial shading [4],[6].

2.1 PV cell single diode equivalent circuit

As illustrated in Figure 4, the PV cell can be implemented by integrating a current source, one exponential diode, and parallel-series equivalent resistance, where V and I represent the terminal voltage and the current. For certain temperature and irradiance, the output current of the solar panel can be calculated as follows:

$$I = N_p[I_{pv} - I_s[e^{\frac{q\left(\frac{V}{N_p}+\frac{IR_S}{N_S}\right)}{kT}} - 1] - \frac{V+IR_S}{R_p}] \quad (1)$$

$$I_{pv} = [(I_{PV,STC} + K_i(T - T_{ref}))\frac{G}{G_{STC}}] \quad (2)$$

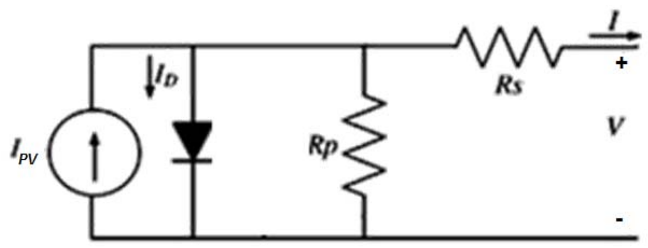

Figure 4. Single diode equivalent circuit of Solar cell

2.2 PV cell double diode equivalent circuit

In the double diode circuit as shown in Figure 5, the solar cell is represented by two exponential diodes. One is an ideal diode, while another is non-ideal.

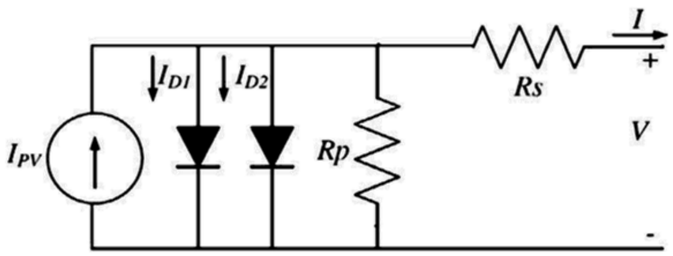

Figure 5. Double diode equivalent circuit of solar cell

$$I = N_p[I_{pv} - I_{D1} - I_{D2} - I_P] \quad (3)$$

$$I_{pv} = [(I_{PV,STC} + K_i(T - T_{ref}))\frac{G}{G_{STC}}] \quad (4)$$

$$I_{D1} = I_{s1}[e^{\frac{q\left(\frac{V}{N_p}+\frac{IR_S}{N_S}\right)}{kT}} - 1] \quad (5)$$

$$I_{D2} = I_{s2}[e^{\frac{q\left(\frac{V}{N_p}+\frac{IR_S}{N_S}\right)}{nkT}} - 1] \quad (6)$$

$$I_p = \frac{V+IR_S}{R_p} \quad (7)$$

where $I_{pv} =$ current generated by incidence light, $R_s, R_P =$ series and shunt equivalent resistance, $I_{D1,D2} =$ diode current, $q = 1.602 * 10^{-19}c$ (electron charge), $K = 1.38 * 10^{-23}J/K(\,boltzmann\ coffieient)$, T =cell surface temperature in Kelvin, T_{ref} =reference temperature in Kelvin, (25°C), K_i =temperature coefficient of SC in percent change per degree, G =irradiance value W/m3, G_{ref} =irradiance nominal value (1000W/m^3), N_s =number of series cells, N_p =number of parallel cells, n = diode quality factor, and $I_{s1,s2}$ =diode saturation current.

3. Perturb and Observe (P&O)

Perturb and Observe is the most commonly used method in practice for its simplicity and ease of implementation [7]-[10]. In this method, the output voltage of the solar panel is perturbed periodically, and then the output power is compared to the previous cycle. Next, corrective action is taken to enforce the voltage to move toward the maximum operation output voltage. The comparison can determine the position of the operation point and the direction of perturbation [11]-[14].

In total, there are three positions and two directions involved. Figure 6 and Table 1 demonstrate the possible positions and directions during the perturbation and observation process and also the required action [15]-[18] in each case to achieve the maximum power output.

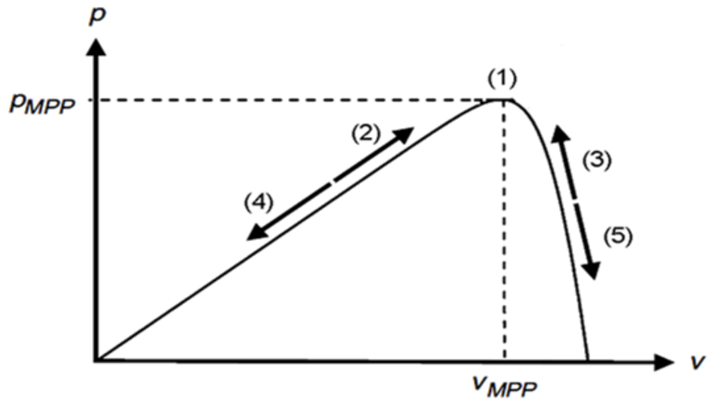

Figure 6. P&O MPPT positioning

Table 1. P&O MPPT positioning and taken action in each case

Position	Variations	Action
1	0dP	No action taken
2	+dP /+dV	increase V
3	+dP /-dV	decrease V
4	-dP /-dV	increase V
5	-dP /+dV	decrease V

4. Proposed variable step size Perturb and Observe

Large step duty cycle has a fast response but experiences noticeable fluctuation around the point of maximum output of a PV module. Meanwhile, small step duty cycle has a slower tracking speed at the start of operation and under dynamic weather, but results in smoother perturbation .The vibration of the large step and the slow speed of associate in power loss are not desired. Benefiting from the high speed of large duty cycles and the soft tracking of the small duty cycle, the proposed variable Perturb and Observe method states that if the perturbation is toward the maximum power point, the duty cycle is increased by multiplication by a factor (A) i.e. $\Delta P>0$. However, if $\Delta P<0$, the duty cycle should be divided by (A), in which this factor is a constant and greater than 1. Figure 7(a) shows the flow chart of the conventional P&O, where fixed duty increment is applied. In Figure 7(b), the flow chart of the proposed technique is presented. In comparison, other variable P&Os, as mentioned in reference [13], utilize two different duty cycles, one is relatively large, used at the beginning of perturbation, and the other is small, used when the system vibrates around maximum power point. This method has a dynamic step size of the duty cycle, which increases its speed, resulting in higher efficiency.

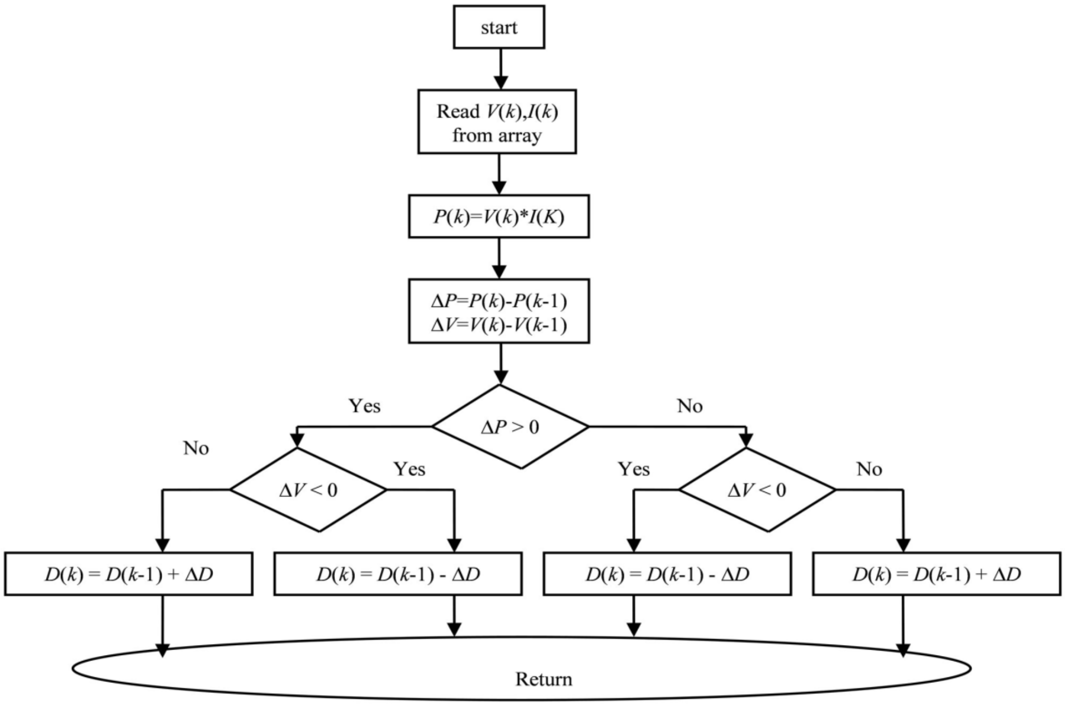

(a)

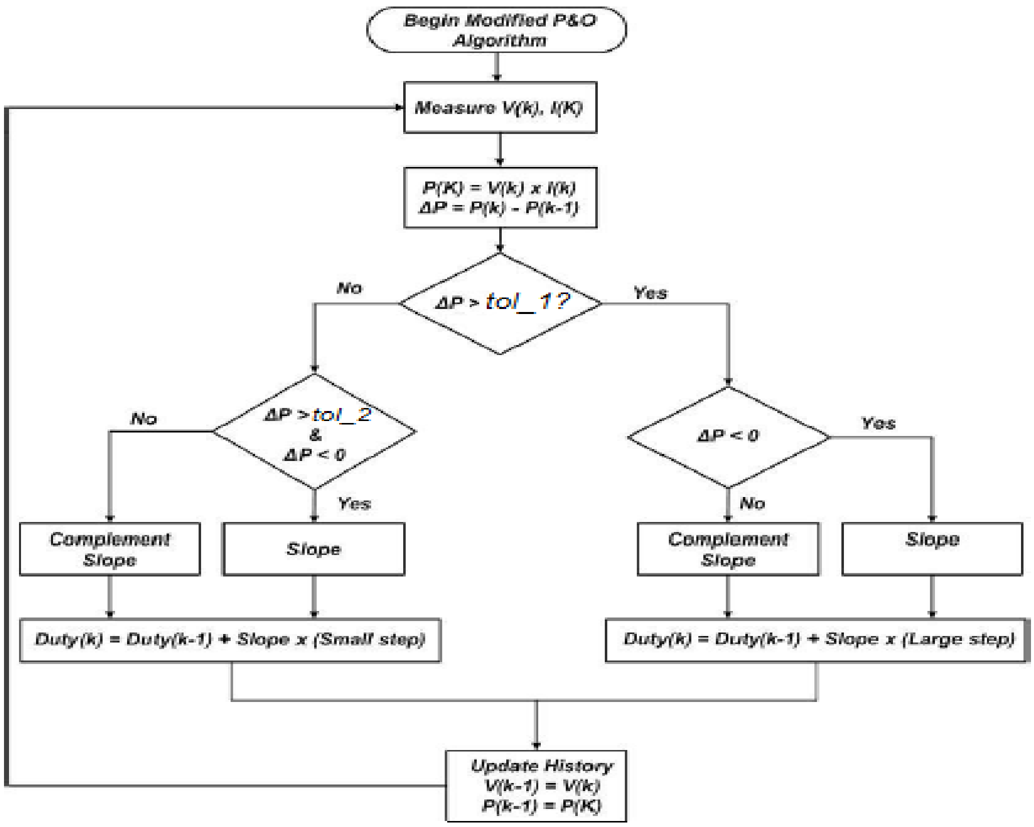

(b)

Figure 7. Flowchart of Perturb and Observe; (a) conventional (b) Modified

5. Simulation and Results

Photovoltaic solar system consists of PV array, switching converter, MPPT controller and load, which may be a DC load, battery charger or inverter. The input(s)/output(s) of MPPT controller may differ from one method to another. Figure 8 shows the block diagram of a typical MPPT system.

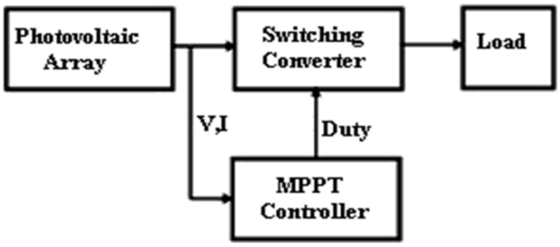

Figure 8. Solar MPPT System

In this study, a 150 W solar panel with the following specification was used in the simulation.

Table 2. PV solar panel data

Parameter	Value
Maximum power (P_{max})	150 W
Voltage at Pmax (V_{MPP})	34.5 V
Current at Pmax (I_{MPP})	4.35 A
Short circuit current (I_{SC})	4.75 A
Open circuit voltage (V_{oc})	40 V
Temparature coefficient of I_{SC}	0.065±0.15%/°C
Temparature coefficient of V_{oc}	-160±20mV/°C
Temparature coefficient of power	-0.5±0.05%/°C
Ideality factor	1.2

In this simulation, boost converter was used to function in continuous current mode. The values of the capacitor and inductor had been calculated for suitable range of duty cycle, and then the highest values were chosen. Table 3 shows the specification of the boost converter's components. Switching frequency of 40 kHz was used slightly above the audiable noise.

Table 3. Boost converter component specification

Parameter	Value
Switching frequency	40 kHz
Inductor	160 µH
Capacitor	65 µF
Load resistance	1000 Ω
Output voltage ripple	0.01V

Figure 9 shows the Simulink model subsystem of double diode modeled PV solar, where the mathematical equation and PV panel parameters are represented. V-I and V-P characteristics of PV module had been determined through open to short-circuit test by ranging the output resistance from zero to infinity.

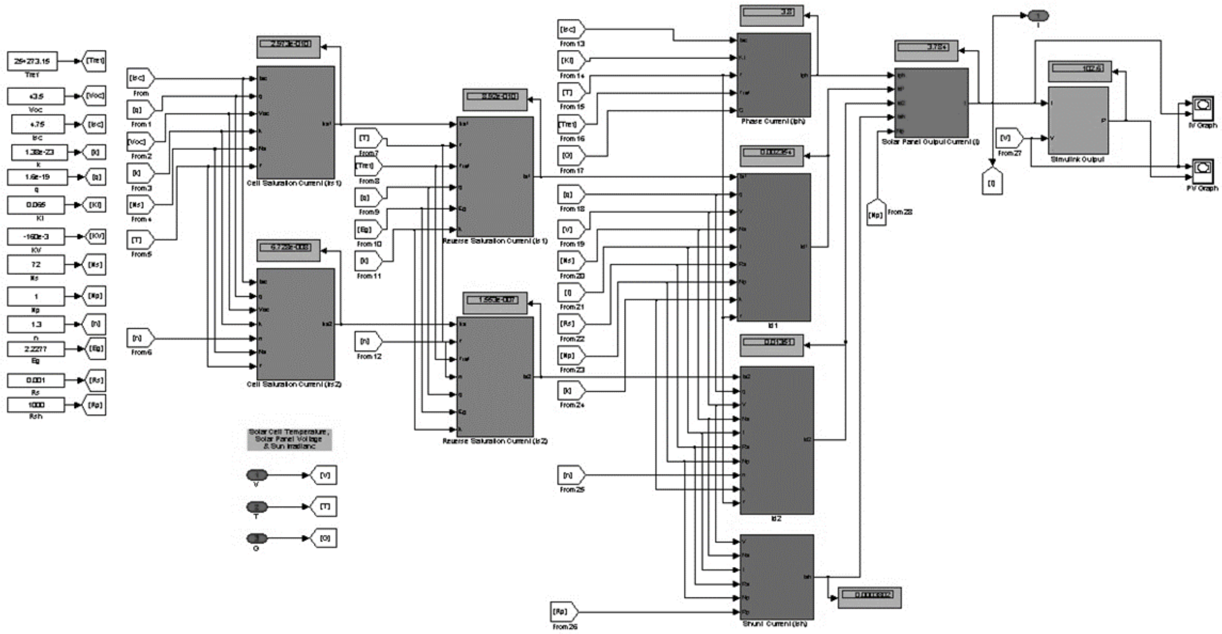

Figure 9. Simulink subsystem of PV module

Figure 10 shows the V-I and V-P characteristic under Standard Test Condition (STC), where G=1000W/m^2 and T=25°C. This result was obtained from the circuit as shown in Figure 9.

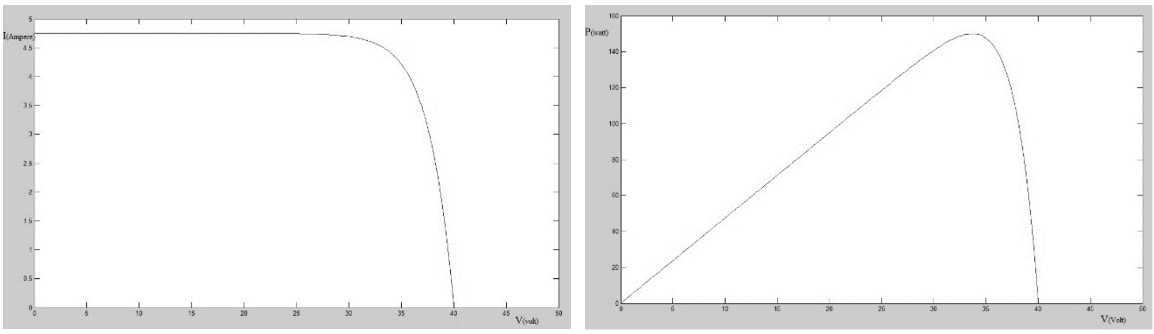

(a) (b)

Figure 10. V-I and V-P characteristic under Standard Test Condition (STC); (a) V-I characteristic of PV module (b) V-P characteristic of PV module

Figure 11 shows the comprehensive system blocks of the solar module, Perturb and Observe algorithm and the switching converter.

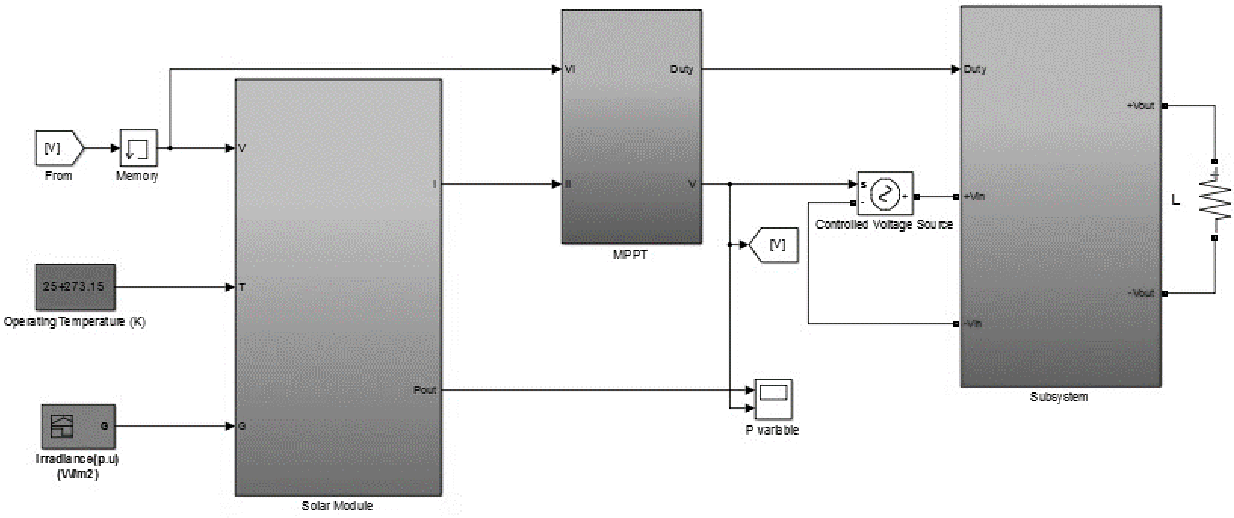

Figure 11. Simulink model of P&O MPPT system

Figure 12 shows the output of large step duty cycle. It had a fast response but also experienced noticable fluctuation around the point of maximum output of a PV module. It took 0.05 m seconds but stabilized at 0.5 milli-second. The vibration of the large step reduced the efficiency, which was not desired.

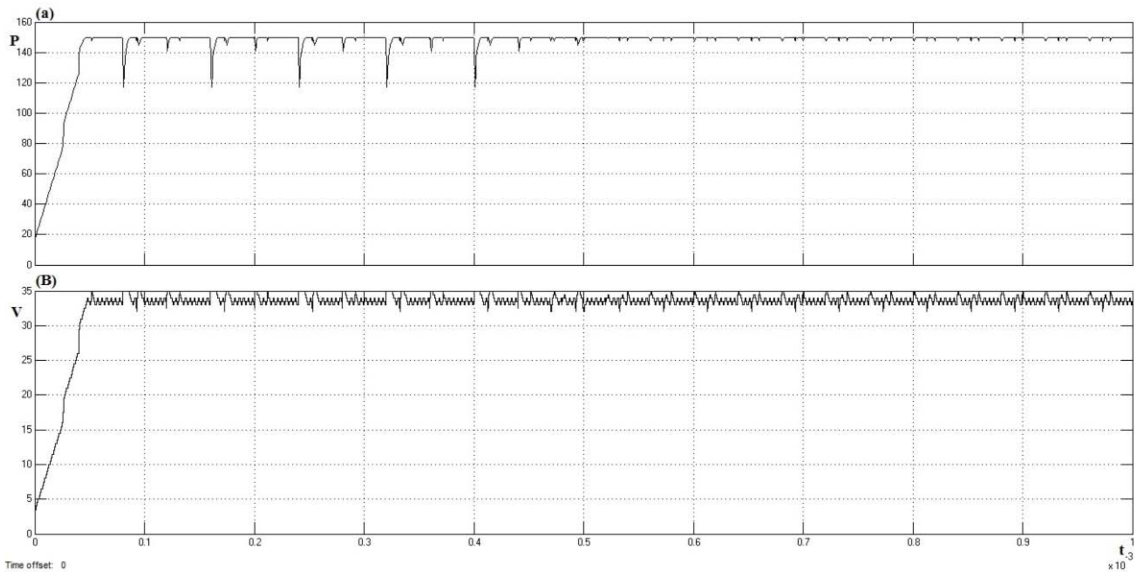

Figure 12. (a) Solar module output power (b) Solar module output voltage
Condition: Duty cycle step of 0.5V, 25°C, unity irradiance

Figure 13 shows the output of small step duty cycle. The small step duty cycle had a slower tracking speed at the start of operation and under dynamic weather, but resulted in smoother perturbation in changing weather at 25°C and unity irradiance. Figure 14 shows the output of the variable step duty cycle P&O at 25°C and unity irradiance. It was observed fluctuating at the beginning of the operation but then rapidly settling. In comparison to the same input as applied in the previous conventional P&O, the variable P&O settled after 0.025 milli-second.

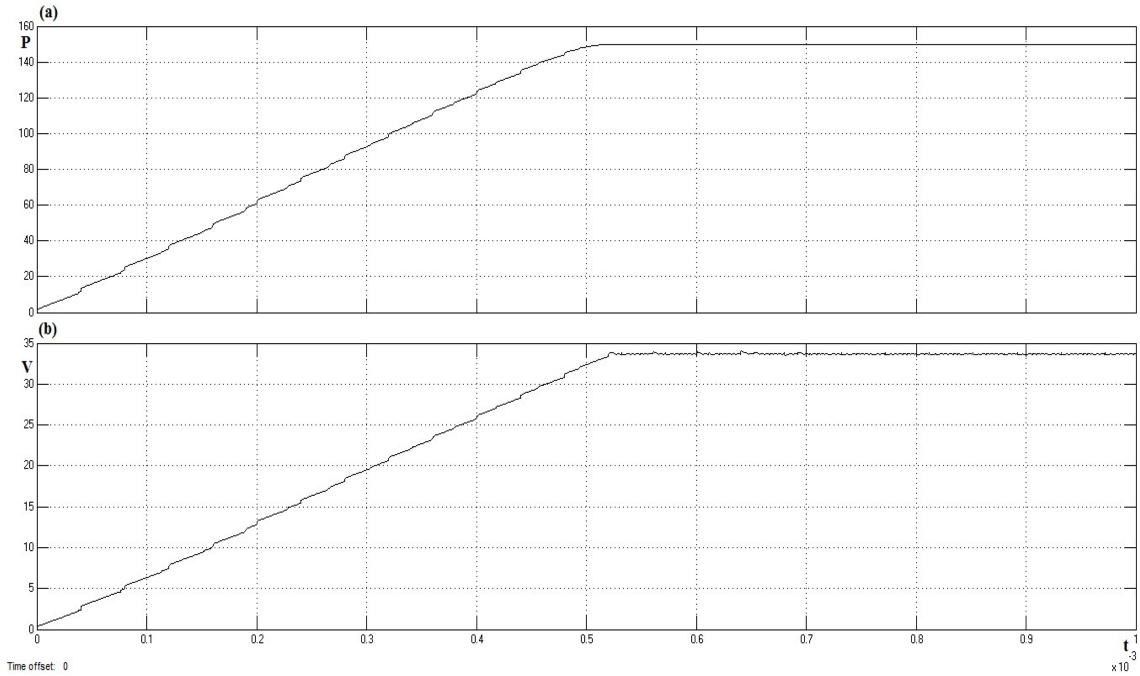

Figure 13. Output of small step duty cycle; (a) Solar module output power (b) Solar module output voltage - condition: duty cycle step of 0.05V, 25°C, unity irradiance

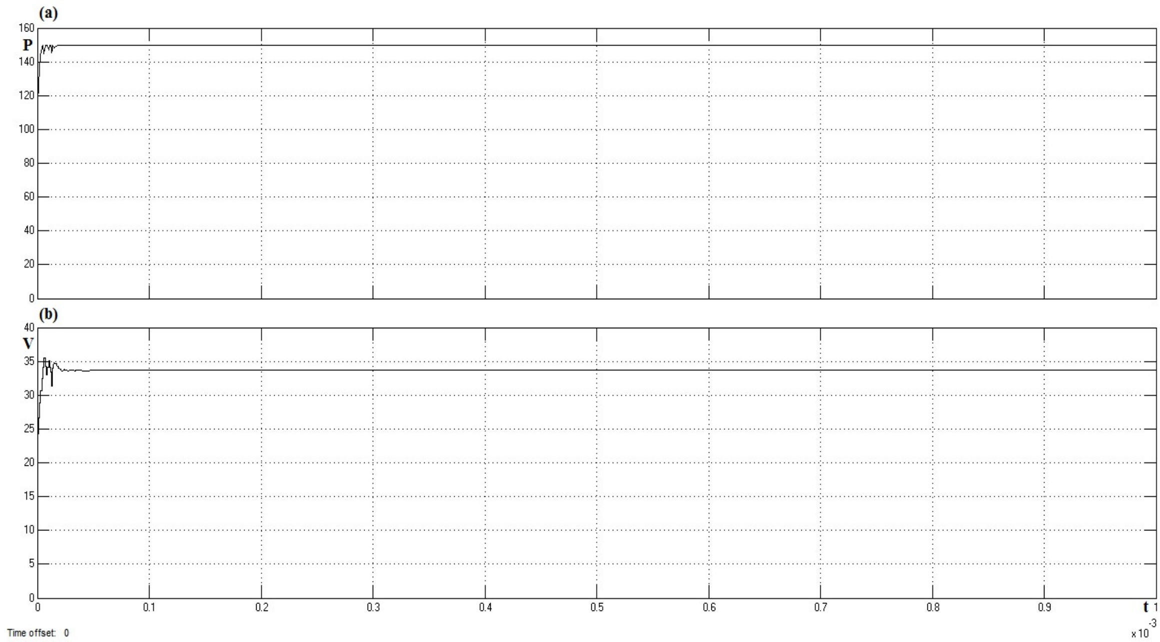

Figure 14. Plot of (a) Solar module output power (b) Solar module output voltage Condition: Variable duty cycle, 25°C, unity irradiance

Figure 15 shows the output of conventional P&O when using large duty cycle, at 25°C and variable irradiance. It was obvious that the system fluctuated dramatically with any irradiance change. This fluctuation was associated with power losses. Figure 16 shows the output of conventional P&O when using small duty cycle, at 25°C and variable irradiance. Here, the system fluctuation was less harsh with any irradiance change. However, the tracking speed was slower, in which the power lost under changing weather.

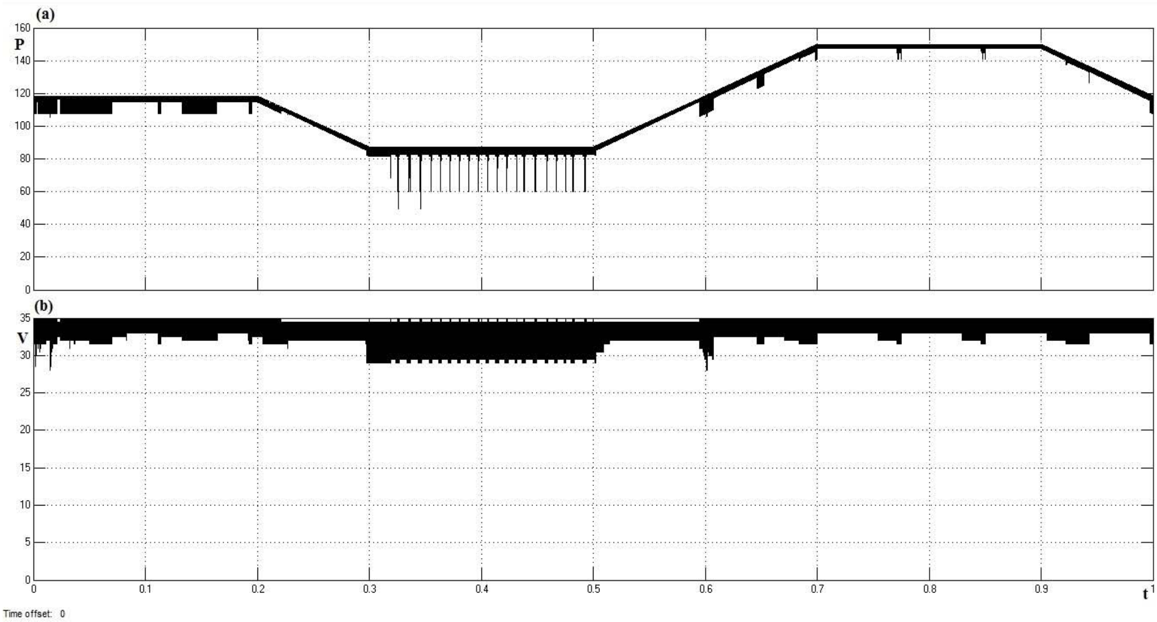

Figure 15. Plot of (a) Solar module output power (b) Solar module output voltage
Condition: Duty cycle step of 0.5V, 25°C, variable irradiance input

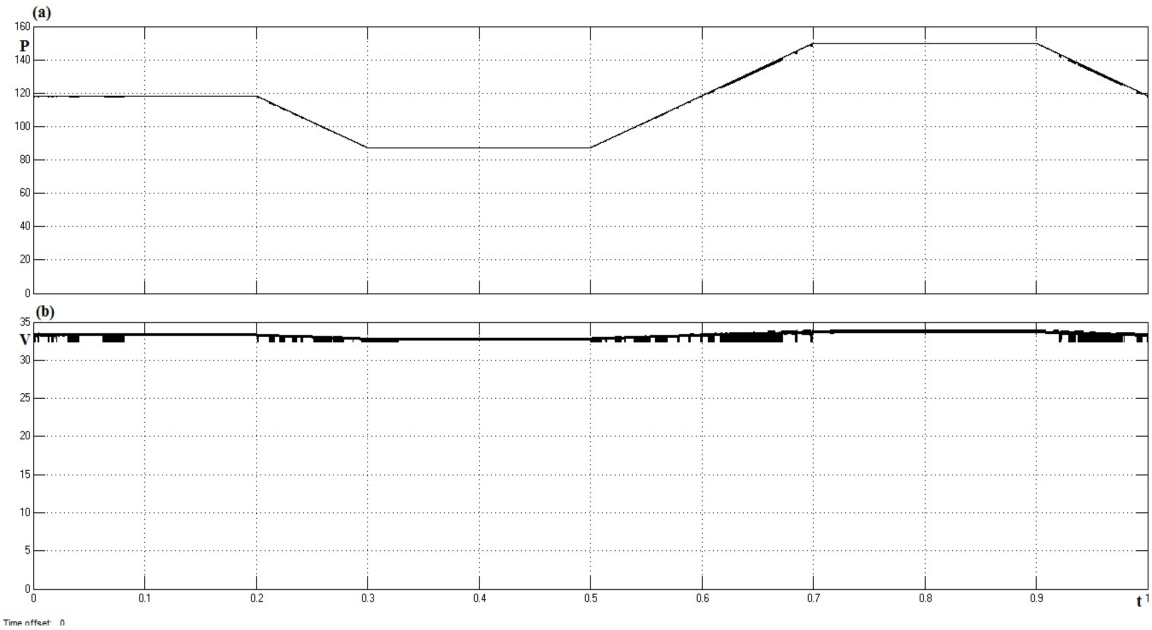

Figure 16. Plot of (a) Solar module output power (b) Solar module output voltage
condition: duty cycle step of 0.05V, 25°C, variable irradiance input

As shown in Figure 17, under fast weather change, variable P&O delivered the best performance, benefiting from the high speed during the first stage of perturbation and fine tuning around the peak power point .

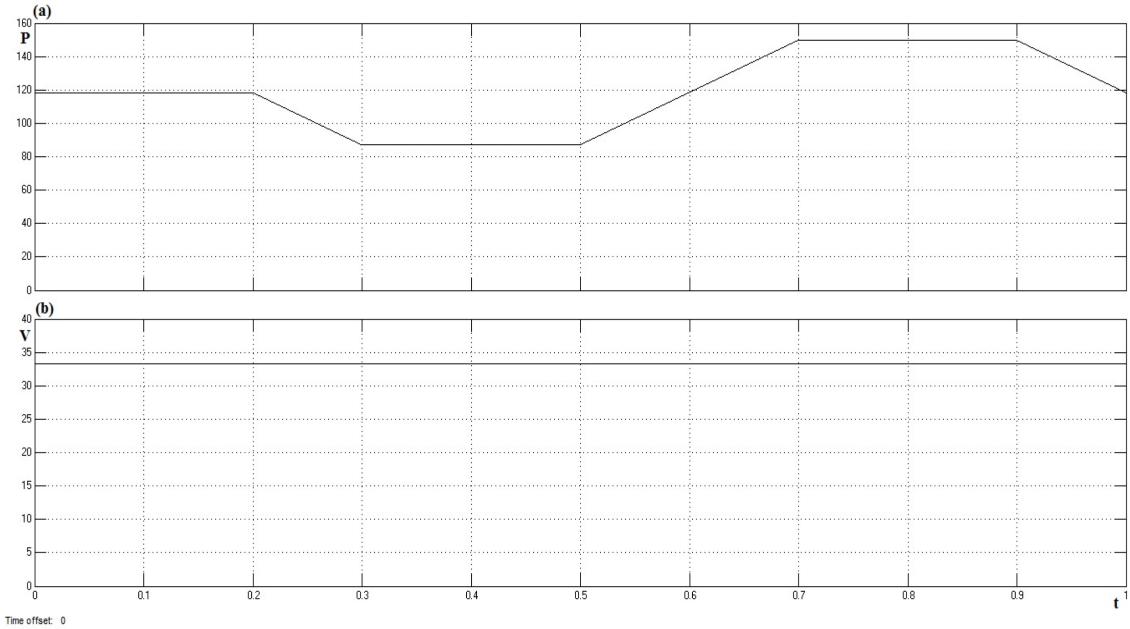

Figure 17. Plot of (a) Solar module output power (b) Solar module output voltage
Condition: A variable duty cycle, 25°C, variable irradiance input

6. Conclusion

In this paper, a new variable step size P&O has been introduced, which shows significant improvement in terms of tracking speed, accuracy and efficiency without additional cost with respect to the conventional P&O MPPT. The proposed modified P&O MPPT has successfully combined the speed of relatively large step size P&O and the smooth tracking of the small step size P&O.

Acknowledgement

The authors would like to express gratitude to Ministry of Education (MOE) and Universiti Teknologi Malaysia (UTM) for the financial support provided under Research University Grant (RUG) Q.J.130000.2523.07H82 and also to Research Management Centre (RMC) for the support and co-operation in the research work.

References

[1] Emilio M, Giovanni P, Giovanni S. Two-steps algorithm improving the P&O steady state MPPT efficiency. *Applied Energy*. 2014; 113: 414–421.
[2] Jancarle LS, Fernando A, Anis C, Cícero CA. Maximum power point tracker for PV systems using a high performance boost converter. *Solar Energy.* 2006; 80(7): 772–778.
[3] Ali AG, Seyed MS, Asma S. A high performance maximum power point tracker for PV systems. *International Journal of Electrical Power & Energy Systems*. 2013; 53: 237–243.
[4] Pallavee B, RK Nema. Maximum power point tracking control techniques: State of art in PV application. *Renewable and Sustainable Energy Reviews*. 2013; 23: 224–241.
[5] Femia N, Petrone G, Spagnuolo G, Vitelli M. *Increasing the efficiency of P&O MPPT by converter dynamic matching*. 2004 IEEE International Symposium on Industrial Electronics. 2004; 2: 1017–1021.
[6] Liu X, Lopes LAC. *An improved perturbation and observation maximum power point tracking algorithm for PV arrays*. Power Electronics Specialists Conference. 2004; 3: 2005–2010
[7] Jusoh A, Sutikno T, Guan TK, Mekhilef A. A Review on Favourable Maximum Power Point Tracking Systems in Solar Energy Application. *TELKOMNIKA Telecommunication, Computing, Electronics and Control*. 2014; 12(1): 6-22.
[8] Hussein KH, Muta I, Hoshino T, Osakada M. *Maximum photovoltaic power tracking: an algorithm for rapidly changing atmospheric conditions*. IEE Proc., Gener. Transm. Distrib. 1995; 142(1): 59–64.

[9] Surya KJ, Sai BCH, Kamalakar BA. Design and analysis of P&O and IP&O MPPT techniques for photovoltaic system. *Int. J. Modern Eng. Res. (IJMER)*. 2012; 2(4): 2174–2180.
[10] Dong J, Zhang CJ, Li YB. *Comparison of duty ratio perturbation & observation and reference voltage perturbation & observation methods applied in MPPT*. Power Electronics and Motion Control Conference (IPEMC). 2012; 2: 1358–1362.
[11] Youngseok J, Junghun S, Gwonjong Y, Choi J. *Improved perturbation and observation method (P&O) of MPPT control for photovoltaic power systems*. Photovoltaic Specialists Conference. 2005: 1788–1791.
[12] Femia N, Petrone G, Spagnuolo GV. *Perturb and observe MPPT technique robustness improved*. 2004 IEEE International Symposium on M. Industrial Electronics. 2004; 2: 845–850.
[13] Mutoh N, Ohno M, Inoue. A Method for MPPT Control While Searching for Parameters Corresponding to Weather Conditions for PV Generation Systems. *IEEE Transactions on T. Industrial Electronics*. 2006; 53(4): 1055–1065.
[14] Khaehintung N, Wiangtong T, Sirisuk P. *FPGA Implementation of MPPT Using Variable Step-Size P&O Algorithm for PV Applications*. International Symposium on Communications and Information Technologies (ISCIT '06). 2006: 212–215.
[15] Fermia N, Granozio D, Petrone G, Vitelli M. Predictive & Adaptive MPPT Perturb and Observe Method. *IEEE Transactions on Aerospace and Electronic Systems*. 2007; 43(3): 934–950.
[16] Femia N, Petrone G, Spagnuolo G, Vitelli M. A Technique for Improving P&O MPPT Performances of Double-Stage Grid-Connected Photovoltaic Systems. *IEEE Transactions on Industrial Electronics*. 2009; 56(11): 4473–4482.
[17] Piegari L, Rizzo R. Adaptive perturb and observe algorithm for photovoltaic maximum power point tracking. *IET Renewable Power Generation*. 2010; 4(4): 317–328.
[18] Ze C, Hang Z, Hongzhi Y. *Research on MPPT control of PV system based on PSO algorithm*. Control and Decision Conference (CCDC). 2010: 887–892.